Design Feature

ZHIHUI HU Engineer
YONGHUA JIANG Professor
XIANG LING Engineer

Naval Aeronautical and Astronautical University, Yantai, People's Republic of China, e-mail: huzhihui226@163.com

UWB Arrays Employ TCAs

These novel phased-array antennas make use of tightly coupled elements with resistive frequency-selective surfaces for outstanding UWB performance.

Low-profile ultrawideband (UWB) phased-array antennas are in great demand for a wide range of commercial and military applications, including in communications, reconnaissance, electronic warfare (EW), and radar systems. Traditional antenna elements for UWB phased-array antennas employ tapered slot, Vivaldi, and rabbit-ear-shaped structures. Although these elements can achieve wide bandwidths, they are not planar for conformal installations and are also too thick for some low-frequency applications.[1-3] Additionally, due to the mutual coupling that occurs between antenna elements in an array layout, the broadband performance can be significantly degraded.

Phased-array antennas based on tightly coupled arrays (TCAs) offer solutions for these diverse applications. A TCA with resistive frequency-selective surface (RFSS) can achieve a wide impedance bandwidth by inserting a square-split-ring RFSS between the array and the ground plane. This suppresses the ground-plane reflections and avoids any short-circuited frequency bands. Simulations have shown that a wide impedance bandwidth of 12.8:1 (with VSWR of less than 2.0:1) can be achieved using a TCA with RFSS.

Without the RFSS, the array exhibits different characteristics across two bands: The scan impedance bandwidth is 8.9:1 (1.8 through 16 GHz) within a ±30° scan angle, and the antenna array's gain is reduced by about 0.5 to 2.8 dB due to the loss of RFSS.

A great deal of interest now surrounds TCAs based on the current sheet concept for wideband applications. Instead of trying to suppress mutual coupling, this approach exploits mutual coupling to counteract ground-plane inductance and maintain a stable, mostly real input impedance over a wide bandwidth. Consequently, a TCA can provide a low profile and UWB operation even if placed over a ground plane.[4-7]

For example, a wideband phased-array antenna with tight coupled octagonal

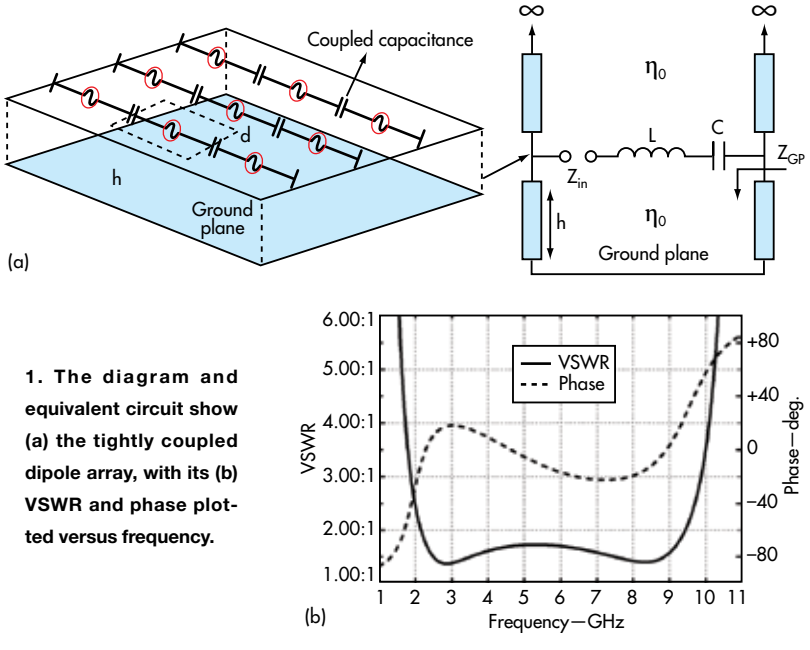

1. The diagram and equivalent circuit show (a) the tightly coupled dipole array, with its (b) VSWR and phase plotted versus frequency.

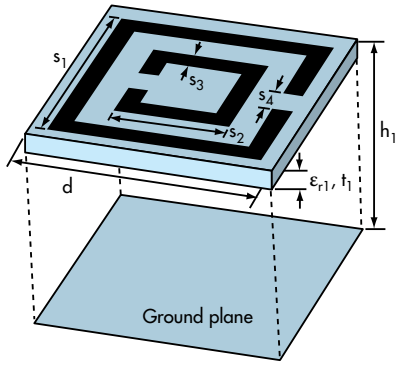

2. The diagram shows a square-split-ring RFSS.

ring elements was presented by Chen,[8] and a 4.4:1 bandwidth with VSWR of less than 2.0:1 was realized. Munk[9] used tightly coupled dipole elements to develop a phased-array structure with wide bandwidth extended to 9:1 with VSWR of less than 3.0:1 by loading multilayer substrates.

Nevertheless, the TCA approach suffers from ground-plane shorting which can severely limit the bandwidth when placed one-half wavelength (λ/2) from the ground plane. To overcome ground-plane shorting, a UWB TCA was designed by inserting a square-split-ring RFSS between the array and the ground plane. To better understand this design approach, the effects of sheet resistivity and mutual coupling on impedance bandwidth were analyzed.

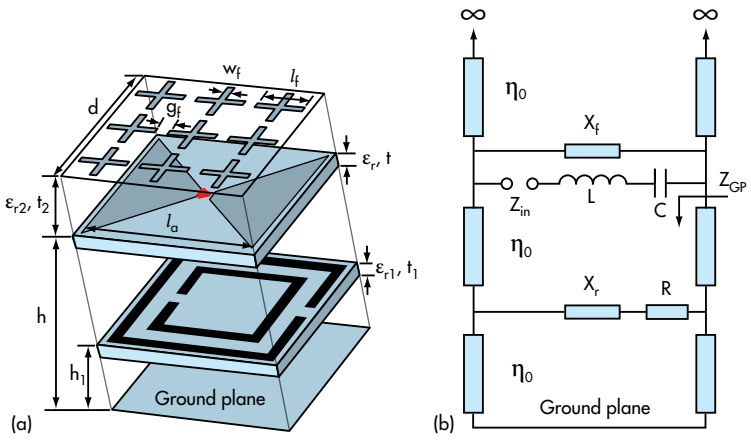

4. The (a) diagram shows a TCA with the RFSS, next to (b) an equivalent circuit.

For this study, a TCA was designed based on the current sheet concept.[10] This design can be described by a tightly coupled dipole array, using the structure and equivalent-circuit model shown in *Fig. 1(a)*. The array is arranged with period, d, and is located a distance, h, from the ground plane. Unlike traditional array elements, the TCA elements are placed within close proximity of each other.

If the end-coupled capacitance is represented by C and the self-inductance of the dipole is denoted by L, the ground plane is represented by a short-circuited transmission line. The impedance looks toward the ground plane equal to Z_{GP}, or

$$Z_{GP} = j\eta_0 \tan(2\pi h/\lambda)$$

and the input impedance of the antenna element, Z_{in}, is

$$Z_{in} = j\omega L + 1/(j\omega C) + \eta_0 \,||\, Z_{GP}$$

where $\eta_0 = 120\pi\omega$ is the characteristic impedance of free space.

Because strong coupled capacitance can counteract ground-plane inductance at the low frequency, the phase of input impedance has a nearly flat response around 0 deg. over a wide bandwidth. As can be seen from *Fig. 1(b)*, a TCA can realize a

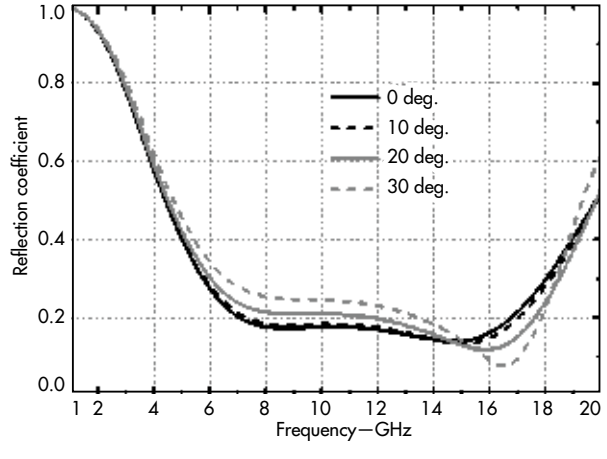

3. The reflection coefficient for the square-split-ring RFSS is plotted versus frequency.

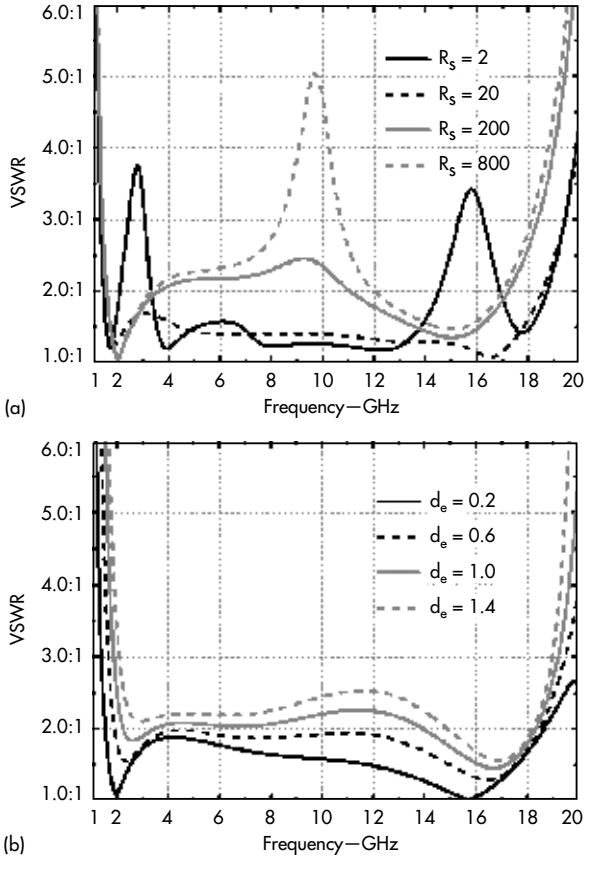

5. These plots show (a) VSWRs with different film resistivities and (b) VSWRs with different element gaps.

4.5:1 (2.1 to 9.5 GHz) bandwidth without substrate loading.

Figure 2 shows a unit cell with square-split-ring RFSS structure. The square-split-ring is comprised of resistive film, with the resistor layer printed on a microwave printed-circuit board (PCB) based on RO4003 circuit substrate from Rogers Corp. (www.rogerscorp.com) with thickness, t_1, of 0.508 mm and dielectric constant, ε_{r1}, of 3.38. The length of the outer square split ring, s_1, is 9.8 mm and the length of the inner square split ring, s_2, is 7.4 mm. The width of both rings, s_3, is 0.6 mm, and the split width, s_4, is 0.6 mm.

When the unit cell with period d = 10.1 mm and resistivity, $R_5 = 33\ \Omega$ is placed a distance $h_1 = 5.5$ mm away from the ground plane, *Fig. 3* shows a simulated reflection coefficient as

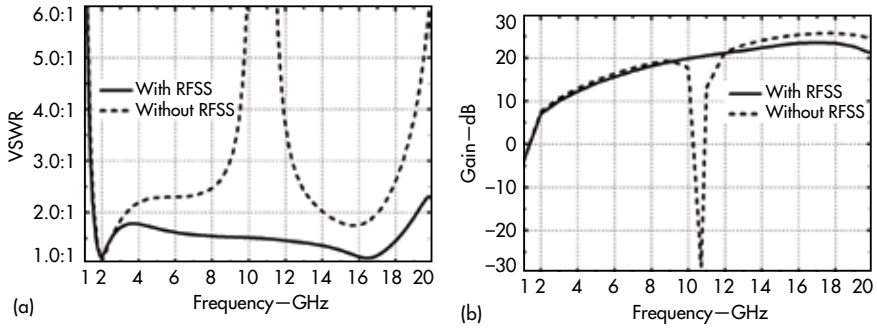

6. The plots show (a) VSWR and (b) gain as functions of frequency.

achieved by means of the Microwave Office simulation software from Computer Simulation Technology (www.cst.com). As these data show, a square-split-ring RFSS can suppress ground-plane reflections over a wide bandwidth.[11]

As can be seen here:

$$Z_{GP} = j\eta_0 \tan(2\pi h/\lambda)$$

the shunt impedance becomes $Z_{GP} = 0$ when $h = \lambda/2$. So, the TCA is short circuited at frequency $f_{max} = c/2h$, severely limiting its bandwidth. To avoid this and increase the TCA bandwidth, an RFSS can be inserted between the TCA and the ground plane.

Figure 4(a) shows a TCA unit cell comprised of a bowtie antenna element, a square-split-ring RFSS, a wide-angle impedance matching (WAIM) layer, and a ground plane. The bowtie antenna element was printed on RO4003 circuit material from Rogers Corp., with thickness, t, of 0.254 mm and dielectric constant, ε_{r1}, of 3.38 placed a distance, h, above the ground plane. A cross WAIM layer with length, l_f, width, w_f, and gap, g_f, was printed on RO4003 circuit material with thickness, t_2, of 4 mm and dielectric constant, ε_{r2}, of 2.2.

Figure 4(b) shows the equivalent-circuit model of the unit cell. It can be seen that the square-split-ring RFSS located a distance, h_1, above the ground plane is represented by resistance R and reactance X_r, while the WAIM layer is represented by reactance X_r, the self-inductance of the bowtie antenna by inductance L, and the coupled capacitance between the adjacent elements by C. Thus, the impedance below the antenna element is:

$$Z_{GP} = \eta_0(1 + \Gamma)/(1 - \Gamma)$$

The input impedance is:

$$Z_{in} = j\omega L + 1/(j\omega C) + \eta_0 \,||\, Z_{GP}$$

where the reflection coefficient is Γ.

The most important parameters for the novel TCA with RFSS are the film resistivity, R_5, and the bowtie antenna element gap, d_e, with $d_e = d - l_a$. To further analyze the effects of such parameters on impedance bandwidth, a TCA with different parameter values was simulated by commercial computer-aided-engineering (CAE) software from CST.

Figure 5(a) shows that the VSWR increases in the middle frequency band as the film resistivity, R_5, increases, while the VSWR increases in the low- and high-frequency bands as film resistivity R_5 decreases. As a consequence, it is very important that a proper value of R_5 be selected for wideband operation.

Figure 5(b) depicts that increasing the element gap leads to higher VSWR. After analyzing the effects of those parameters, optimized parameter values were achieved. The film resistivity is $R = 50\ \Omega$, and the other values are shown in the *table*.

Based on the aforementioned parameter values, a 10 x 10 TCA was modeled using commercial CAE simulation software. *Figures 6(a)* and *(b)* depict the VSWR and gain of the TCA with and without the RFSS. As can be seen, the impedance bandwidth with the RFSS can achieve a bandwidth of 12.8:1 (1.5 to 19.2 GHz), while without the RFSS, the performance is sectioned into two bandwidths.

Figure 6(b) shows that the gain decreases drastically at 10.7 GHz without the RFSS, corresponding to the short-circuited frequency point, while a wide bandwidth is maintained with the RFSS. Without the RFSS, the gain of the antenna array is reduced by 0.5 to 2.8 dB.

The normalized E- and H-plane radiation patterns were plotted at 1.5, 10.7, and 19.2 GHz (data are available in the online version of this article at mwrf.com/passive-

components/uwb-arrays-employ-tcas). In the mainlobe direction, the pattern exhibits a null at 10.7 GHz without the RFSS. With the RFSS, the null is suppressed, indicating the suppression of ground-plane shorting. The impedance bandwidth is 1.5 to 19.2 GHz for a scan angle of 0 deg. As the scan angle increases, the VSWR also increases and the impedance bandwidth decreases. The TCA can be used to realize an impedance bandwidth of 8.9:1 within a ±30-deg. scan angle.

The copolarized and cross-polarization patterns with scan angles of 0, ±10, ±20, and ±30 deg. at 10.7 and 19.2 GHz indicate stable performance at those frequencies (plots are available in the online version of this article. It is reasonable to conclude that the radiation of TCA with RFSS is stable over whole bandwidth within the ±30 deg. scan angle, the sidelobe level is below −10 dB, and the cross-polarization level is below −40 dB.

Because of the metal ground planes in many antenna arrays, a TCA can be short circuited at a particular frequency, limiting its impedance bandwidth. To solve this problem, a TCA was designed with an RFSS. Using a TCA with a tightly coupled bowtie antenna as its radiation element, the impedance bandwidth was greatly improved by inserting an RFSS between the array and ground plane.

Simulated results show that the impedance bandwidth of the TCA with RFSS was 12.8:1 (1.5 to 19.2 GHz), while without the RFSS, the impedance bandwidth was split into two bands. In these bands, the scan impedance bandwidth was 8.9:1 (1.8 ~ 16 GHz) with a scan angle of ±30 deg. The sidelobe levels were below −10 dB, the cross-polarized levels were below −40 dB, and the gain of antenna array was reduced by 0.5 to 2.8 dB without the RFSS. The TCA with the RFSS offers broad bandwidth, low profile, and easily conformal installation, and is well suited for UWB phased-array antenna systems. MW

REFERENCES

1. A. Ellgardt, "A Scan Blindness Model for Single-Polarized Tapered-Slot Arrays in Triangular Grids," IEEE Antennas and Wireless Propagation Letters, Vol. 11, 2011, pp. 117-120.
2. A. Ellgardt and A. Wikstrom, "A Single Polarized Triangular Grid Tapered-Slot Array Antenna," IEEE Transactions on Antennas and Propagation, Vol. 57, No. 9, 2009, pp. 2599-2607.
3. Y. Yao, M. Liu, and W. Chen, "Analysis and design of wideband widescan planar tapered slot antenna array," IET Microwave Antennas and Propagation, Vol. 4, No. 10, 2010, pp. 1632-1638.
4. S.S. Holl and M.N. Vouvakis, "The planar ultra-wideband modular antenna array," IEEE Transactions on Antennas and Propagation, Vol. 60, No. 1, 2012, pp. 130-140.
5. E.A. Alwane, K. Sertel, and J.L. Volakis, "A simple equivalent circuit model for ultrawideband coupled arrays," IEEE Antennas and Wireless Propagation Letters, Vol. 11, 2011, pp. 117-120.
6. J.L. Volakis and K. Sertel, "Narrowband and wideband metamaterial antennas based on degenerate band edge and magnetic photonic crystals," IEEE Proceedings, Vol. 99, No. 10, 2011, pp. 1732-1745.
7. I. Tzanidis, K. Sertel, and J. L. Volakis, "Characteristic excitation taper for ultrawideband tightly coupled antenna arrays," IEEE Transactions on Antennas and Propagation, Vol. 58, No. 11, 2012, pp. 1777-1784.
8. Y. Chen, S. Yang, and Z. Nie, "A novel wideband antenna array with tightly coupled octagonal ring elements," Progress In Electromagnetic Research, Vol. 124, 2012, pp. 55-70.
9. B. Munk, R. Taylor, and T. Durham, "A low-profile broadband phased array antenna," Proceedings of Antennas and Propagation Society International Symposium, IEEE Press, Columbus, OH, 2003, Vol. 2, pp. 448-451.
10. H.A. Wheeler, "Simple relations derived from a phased-array antenna made of an infinite current sheet," IEEE Transactions on Antennas and Propagation, Vol. 13, 1965, pp. 506-514.
11. Y.E. Eredmli, K. Sertel, and J.L. Volakis, "Frequency selective surfaces to enhance performance of broadband reconfigurable arrays," IEEE Transactions on Antennas and Propagation, Vol. 50, No. 12, 2002, pp. 1716-1724.

KEY PARAMETERS AT A GLANCE.

Parameter	d	d_e	h	l_a	g_a	l_f	w_f	g_f
Value (in mm)	10.1	0.2	14	9.9	0.4	2.53	0.3	0.84

PARAMETER VALUES (UNIT: mm).

d	d_e	h	l_a	g_a	l_f	w_f	g_f
10.1	0.2	14	9.9	0.4	2.53	0.3	0.84